208 *Macromolecules* **1987,** *20,* 208-211

Rheological and Thermal Properties of Poly(methylalkylsiloxane)

Peter B. Rim,* Husam A. A. Rasoul, Steven M. Hurley, E. Bruce Orler, and Kevin M. Scholsky

Louis Laboratory, S. C. Johnson & Son, Inc., Racine, Wisconsin 53403.

Received June 23, 1986

ABSTRACT: The solution viscosity, steady-shear melt rheology, and thermal properties of a series of poly(methylalkylsiloxanes) of varying alkyl length have been investigated. For a given main-chain molecular weight, both the intrinsic viscosity and the melt viscosity were observed to increase with increasing side-chain molecular weight. The solution and melt viscosity data were analyzed with classical relations given by Flory and Rouse, respectively. Calorimetric and X-ray diffraction results show that the alkyl side chains are crystallizable and exist in the hexagonal unit cell. The extended-chain equilibrium melting point of the side chains was determined, from a Hoffman-Weeks plot, to be 140 °C, and an equilibrium heat of fusion of 222 J/g was calculated.

Introduction

There has been a renewed interest in the area of polymers with crystallizable side chains in this and other laboratories.[1-10] Recent work in our group has been concerned with the properties of a series of poly(α-olefin-*co*-maleic anhydride) materials with varying α-olefin side-chain length.[7-10] The thermal properties[7] and kinetics of polymerization[8] and hydrolysis[9] have been investigated.

The inherent molecular architecture of comblike materials can result in some rather interesting properties. For example, if the main chain is amorphous and contains relatively "stiff" monomers, as is the case for the α-olefin/maleic anhydride copolymers, the main-chain glass transition temperature (T_g) can be greater than the side-chain melting point (T_m).[7] The influence of a high T_g is to decrease the crystallizability of the side chains. A general model that predicts this decreased crystallizability has been developed.[10]

In this paper the properties of a series of poly(methylalkylsiloxanes) of varying alkyl side-chain length will be discussed. For a given side-chain length, these materials differ greatly from the α-olefin/maleic anhydride copolymers because of the high flexibility of the main chain. This system offers an excellent opportunity to unambiguously measure the influence of alkyl side-chain length on properties because the polymers are prepared by "adding" an α-olefin to an existing poly(methylhydrosiloxane), thereby eliminating any effects due to main-chain molecular weight differences.

The properties of interest are the dilute solution viscosity, steady-shear melt viscosity, and thermal properties. In all cases, care has been taken to ensure the absence of residual α-olefin because of the potential influence of this variable on the resultant properties. For short α-olefins this was performed by usual distillation procedures, and for α-olefins of $\geq$16 carbons supercritical fluid fractionation was employed.[11,12]

Experimental Section

1. **Synthesis.** Synthesis of the poly(methylalkylsiloxanes) was performed by a hydrosilation reaction of poly(methylhydrosiloxane) (Polysciences, Inc.) and α-olefins of varying length available from Aldrich. The number-average molecular weight of the precursor siloxane polymer was determined by vapor-phase osmometry to be 3020. A three-necked round-bottomed flask equipped with a thermometer, a mechanical agitator, and a nitrogen purge was charged with a 50% solution (w/w) of the reactants (14% molar excess α-olefin) in dry toluene. Hydrogen hexachloroplatinate(IV) (150 ppm) was then added to the purged reaction mixture, which was maintained at 60 °C for 3 days. The reaction mixture was filtered to remove the catalyst, refluxed with activated charcoal for 1 h, and filtered hot through a filter aid available from Johns-Manville Corp. Finally, the solvent was removed under reduced pressure. The reactions proceeded to completion as evidenced by the absence of the Si-H absorption at 2130 cm^{-1} in the infrared spectra.

Table I
Molecular Weight (GPC) and Residual α-Olefin Data

polymer	n_c	M_n	M_w	residual α-olefin, wt %
poly(methyloctylsiloxane)	8	5400	22 250	0.01
poly(methylnonylsiloxane)	9	5730	23 890	<0.01
poly(methyldecylsiloxane)	10	6400	24 750	<0.01
poly(methylundecylsiloxane)	11	7270	25 360	<0.01
poly(methyldodecylsiloxane)	12	6330	23 590	0.53
poly(methyltetradecylsiloxane)	14	7180	25 230	0.86
poly(methylhexadecylsiloxane)	16			<0.30
poly(methyloctadecylsiloxane)	18			0.32
poly(methyleicosanylsiloxane)	20			0.89

2. **Purification.** Excess α-olefin of length $\leq$14 carbons was removed under a vacuum of 0.5 mmHg at 100 °C. Polymers prepared with longer α-olefins were purified by a supercritical fluid fractionation (SCF) technique using nitrous oxide at temperatures and pressures ranging from 50 to 100 °C and 1100 to 7000 psi, respectively. The bulk of unreacted monomer was removed by processing at 1100-2000 psi, and the purified polymer was obtained by extracting at pressures of 3000-7000 psi. Because the SCF procedure resulted in fractionation with respect to polymer molecular weight as well as α-olefin removal, only the materials purified by vacuum were used in the solution and melt viscosity studies.

3. **Molecular Weight Determination.** Molecular weights relative to polystyrene standards were determined by gel permeation chromatography (GPC). The system consisted of a Spectra Physics isocratic pump, four μStyragel columns (100, 10^3, 10^4 and 10^5 Å; Waters Associates, Inc.), an R401 differential refractometer detector, and an IBM 9000 computer to facilitate data storage and handling. The calibration curve was determined by fitting a third-order polynominal to a plot of log (molecular weight) vs. retention time. Tetrahydrofuran (THF) was used as the mobile phase at a flow rate of 0.7 mL/min. The results of the GPC analysis are summarized in Table I.

4. **Residual Monomer Analysis.** A Tracor 565 gas-liquid chromatograph with a flame ionization detector and a 30-m Megabore column (100% methylpolysiloxane stationary phase, J& W Scientific Inc.) was used to determine the concentration of residual α-olefin in the purified polymers (Table I). The analysis procedure consisted of an initial temperature of 60 °C with a 2-min hold, followed by a linear ramp at 6 °C/min to 200 °C. Nitrogen was used as the carrier gas, and an IBM 9000 was employed for data analysis. Samples were prepared for analysis by dissolving quantitative amounts of the specimen and decafluorobiphenyl (internal standard) in THF.

5. **Viscosity Measurements.** Solution viscosities were determined in toluene at 30 °C by using an Ubbelohde viscometer. Melt viscosities were obtained by using a Bohlin rheometer (Bohlin Rheology A.B.) at 25 °C employing shear rates from 0.371 to 371 s^{-1}.

0024-9297/87/2220-0208$01.50/0 © 1987 American Chemical Society

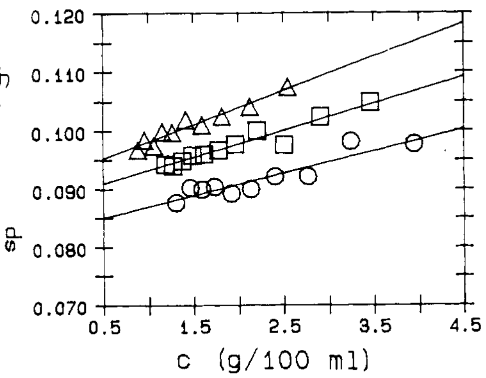

Figure 1. Plot of η_{sp}/c vs. c for representative poly(methylalkylsiloxanes): (○) $n_c = 8$; (□) $n_c = 11$; (△) $n_c = 14$.

Table II
Solution Viscosity Data

n_c	$[\eta]$, dL/g	$M_n{}^a$	$(\bar{r}^2)^{1/2} \times 10^7$, cm
8	0.0832	8658	6.90
9	0.0875	9362	7.20
10	0.0834	10067	7.27
11	0.0886	10772	7.58
12	0.0901	11476	7.79
14	0.0924	12886	8.16

[a] Calculated from precursor M_n.

6. Thermal Analysis. Differential scanning calorimetry (DSC) was performed with a Du Pont 910 DSC module/1090B thermal analyzer at a heating rate of 20 °C/min. Indium was used as a calibration standard for heats of fusion (ΔH_f's), and both indium and high-purity water were used to correct the T_m's for instrument offset. Sample sizes ranged from 2 to 4 mg, and T_m's are cited as the peak onset, determined by extrapolation of the leading edge of the endotherm to the base line.

Results and Discussion

1. Dilute Solution Viscosity. In Figure 1 is plotted η_{sp}/c vs. c (η_{sp} is the specific viscosity) for representative poly(methylalkylsiloxanes) dissolved in toluene. The intercept yields the intrinsic viscosity ($[\eta]$) according to the Huggins equation[13]

$$\eta_{sp}/c = [\eta] + k[\eta]^2 c \qquad (1)$$

where k is a constant. Values of $[\eta]$ determined from least-squares fits of the Huggins plots are depicted in Figure 2 and given in Table II as a function of side-chain length (n_c). The $[\eta]$ increases with increasing side-chain length. In order to evaluate this behavior we consider a relation given by Flory for the Θ-condition[13,14]

$$[\eta] = \Phi(\bar{r}^2)^{3/2}/M \qquad (2)$$

where $[\eta]$ is the intrinsic viscosity (dL/g), Φ is a universal constant $\approx 2.2 \times 10^{21}$, $(\bar{r}^2)^{1/2}$ is the root-mean-square end-to-end distance of the solute (cm), and M is the molecular weight.

Since all of the materials were synthesized from the same main-chain precursor, M increases with increasing side-chain molecular weight. Because of precautions taken during synthesis and purification, we are confident that no variation in molecular weight or molecular weight distribution occurred other than those attributable to side-chain addition. In addition, the infrared spectroscopy results discussed in the Experimental Section indicate that side-chain addition was complete. Therefore, we can calculate M_n for all of the materials studied from the precursor M_n (Table II). From the $[\eta]$ and M_n data, and assuming the Θ-condition, we have calculated the number-average root-mean-square end-to-end distance $(\bar{r}^2)^{1/2}$ according to eq 2 (Table II). The number-average value, which is preferred when studying polydisperse samples,[13,14] increases with increasing side-chain length. Increases in $(\bar{r}^2)^{1/2}$ result from increases in M, increases in inherent chain rigidity, or increases in solubility characteristics. It is impossible at this time to comment on the exact contribution of each of these factors. It should be noted that the assumption of a Θ-condition is probably not valid as evidenced by the low slope of the η_{sp}/c vs. c plots[15] (Figure 1). This will not alter the relative importance of our calculations.

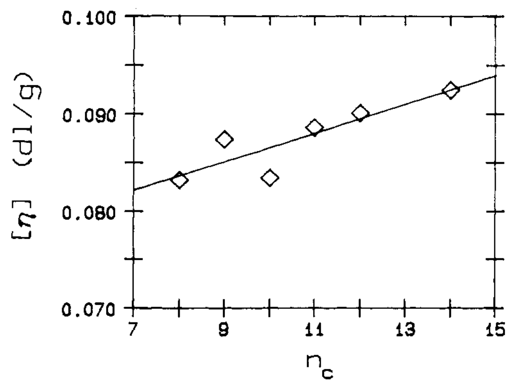

Figure 2. Plot of intrinsic viscosity $[\eta]$ vs. side-chain length (n_c).

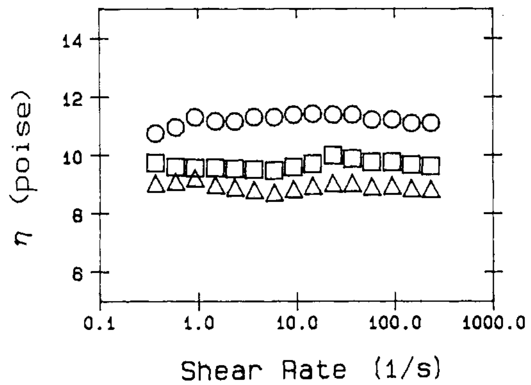

Figure 3. Plot of steady-shear melt viscosity (η) vs. shear rate for representative poly(methylalkylsiloxanes): (△) $n_c = 9$; (□) $n_c = 10$; (○) $n_c = 12$.

Comparison of the calculated M_n's to the GPC-derived M_n's indicates that use of the polystyrene-based GPC values results in a serious underestimation of molecular weight. This occurs because of hydrodynamic volume differences between polystyrene and the siloxane polymers at constant molecular weight arising from solubility differences or the comblike nature of the poly(methylalkylsiloxanes).

2. Melt Viscosity. Figure 3 depicts the steady-shear melt viscosity (η) as a function of shear rate for representative poly(methylalkylsiloxanes). All of the materials were observed to behave as Newtonian fluids over the shear rates monitored. The viscosity data, which is plotted as a function of side-chain length in Figure 4, exhibit an increase with increasing side-chain length. This increased viscosity can be envisioned to result from the increased molecular weight (i.e., $\bar{r}^2$) with increasing side-chain length or from increased inherent resistance to flow (i.e., monomeric frictional coefficient). The following relationship, which results from a modified Rouse model appropriate for materials with M less than the entanglement M, can be used to determined the monomeric frictional coefficient[16,17] (ζ_0)

$$\zeta_0 = 36M_0\eta_0/(\rho\bar{r}^2N_0) \qquad (3)$$

where M_0 is the monomer molecular weight, η_0 is the

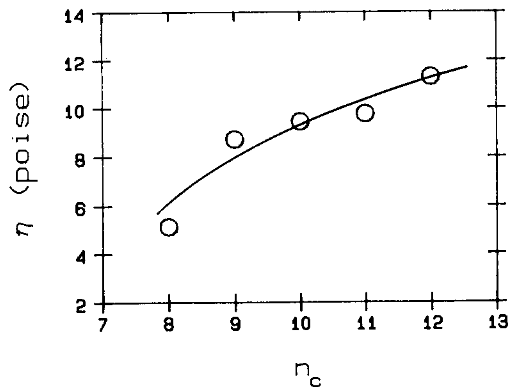

Figure 4. Plot of steady-shear melt viscosity (η) vs. side-chain length (n_c).

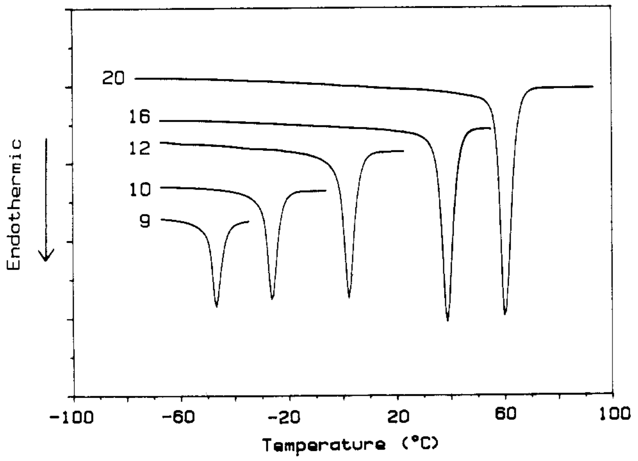

Figure 5. Representative DSC traces of poly(methylalkylsiloxanes). Curve designations correspond to n_c, and the curves have been shifted vertically for clarity.

Table III
Melt Viscosity Data

n_c	η, P	ρ, g/cm^3	log ζ_0, dyn·s/cm
8	5.11	0.8990	−6.91
9	8.73	0.8988	−6.68
10	9.47	0.8931	−6.62
11	9.77	0.8891	−6.61
12	11.30	0.8867	−6.54

zero-shear viscosity, ρ is the density, $\bar{r^2}$ is the mean-square end-to-end distance, and N_0 is Avogadro's number.

Table III summarizes the values of ζ_0 calculated by using the η and ρ data in Table III and the $\bar{r^2}$ values from Table II. Use of the dilute solution values of $\bar{r^2}$ is considered an approximation, which should not alter the relative nature of the calculations. The results indicate that ζ_0 increases with increasing side-chain length, in contrast to the behavior observed for other comblike polymers. In these previous studies, which were performed on materials with rigid main chains and flexible side chains, the pendant chains were envisioned to cause the main chain to become more flexible via a free volume effect.[16,18] In our system the side chains apparently stiffen the relatively flexible backbone. Therefore, the increase in viscosity with increasing side-chain length is the result of increases in both $\bar{r^2}$ and ζ_0.

3. Thermal Analysis. Figure 5 depicts DSC traces of representative poly(methylalkylsiloxanes) that have been cooled from the melt at 10 °C/min prior to analysis at a heating rate of 20 °C/min. The endotherm evident for each trace is associated with the melting of the paraffinic side chains. No evidence for main-chain crystallinity or glass transition temperatures (T_g's), which are believed to occur at temperatures less than −100 °C, was observed. The side-chain T_m's and heats of fusion (ΔH_f's), normalized for side-chain weight fraction, are plotted as a function of n_c in Figures 6 and 7, respectively. As expected, both increase with increasing side-chain length.[7,19] The melting point data, although somewhat high, are in best agreement with previously published data for paraffins in the hexagonal unit cell, which is commonly referred to as the "rotator" phase.[20] Preliminary powder X-ray diffraction studies on the polymers with $n_c = 18$ and $n_c = 20$ support this argument because of the presence of a single diffraction maxima corresponding to $d = 4.06$ Å.[1-3,21] For a given side-chain length, the T_m's and ΔH_f's of the siloxane polymers are considerably higher than those previously measured for the α-olefin/maleic anhydride system.[7] This occurs because the increased mobility of the siloxane main chain allows crystallization to proceed with little or no inhibition.[10,22] According to the Gibbs–Thomson expression,[23] the intercept of a plot of T_m vs. $1/n_c$, such as depicted in Figure 6, yields a value of the equilibrium melting point ($T_m°$)

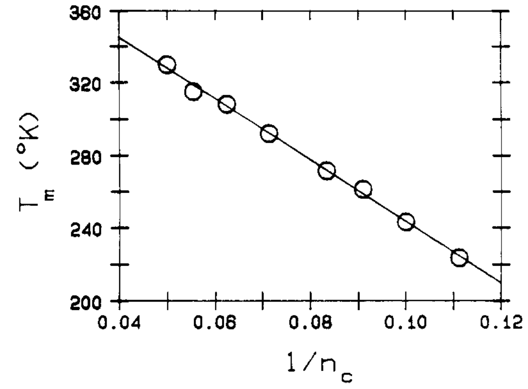

Figure 6. Plot of side-chain melting point (T_m) vs. $1/n_c$.

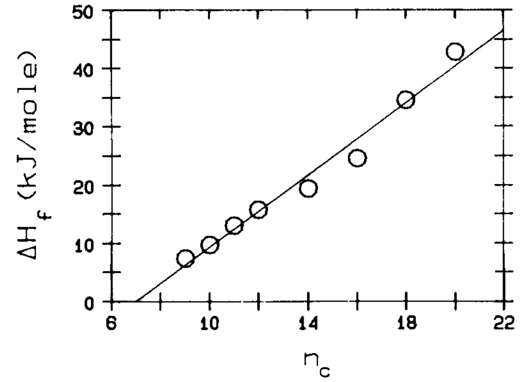

Figure 7. Plot of side-chain heat of fusion (ΔH_f) vs. n_c.

$$T_m = T_m°\left(1 - \frac{2\sigma_e}{\Delta H_f° l}\right) \tag{4}$$

where $T_m°$ is the equilibrium melting point, σ_e is the end surface energy of the crystal, $\Delta H_f°$ is the equilibrium heat of fusion, and l is the crystal thickness. Analysis of the plot results in a value of 140 °C for $T_m°$, which should be considered specific for the hexagonal unit cell. This value is close to that of 141.6 °C obtained for the orthorhombic modification by Wunderlich.[24] However, the accuracy of our result should be questioned because of the rather long extrapolation. In addition, $T_m°$ values have been experimentally and theoretically predicted for both unit cells to be some 5 °C higher than our value.[25,26] The Flory–Vrij approach,[25] which is another way to determine $T_m°$ from low molecular weight analogues, has not been employed because the narrow range of side-chain lengths in this investigation again decrease the significance of the analysis. The ΔH_f data of polymers with crystallizable side chains has been frequently described by the relationship[3,22,27]

$$\Delta H_f = \Delta H_{fe} + n_c k \quad (5)$$

where ΔH_f is the observed heat of fusion per mole, ΔH_{fe} is the chain-end contribution to enthalpy, and $k = \Delta H_f°$ per mole of CH_2.

The slope (k) of the ΔH_f vs. n_c plot, depicted in Figure 7, yielded a $\Delta H_f°$ value of 3.1 kJ/mol (222 J/g) for our materials. This value is indicative of a hexagonal unit cell and is extremely close to those determined by other researchers.[3,22] Equilibrium heats of fusion for other potential unit cells are considerably higher.[20,24] Studies are planned to prepare materials with longer paraffin side chains to increase the accuracy of the extrapolation to equilibrium.

Conclusions

1. The intrinsic viscosity in toluene of poly(methylalkylsiloxanes) of a given main-chain molecular weight was observed to increase with increasing side-chain molecular weight. This behavior is interpreted in terms of an increase in hydrodynamic volume with increasing side-chain length. Reasonable values of the mean-square end-to-end distance have been calculated.

2. The steady-shear melt viscosity of the same set of materials was also observed to increase with increasing side-chain length. Increases in the mean-square end-to-end distance and the monomeric frictional coefficient with increasing side-chain molecular weight are responsible for this trend.

3. DSC studies show that the alkyl side chains of these materials are crystallizable and that both the melting point and the heat of fusion increase with increasing side-chain length. X-ray diffraction results indicate that the side chains crystallize in the hexagonal unit cell. Values for the equilibrium melting point and equilibrium heat of fusion of the side chains have been determined to be 140 °C and 222 J/g, respectively.

Acknowledgment. We thank S. Determan for preparing this manuscript, J. P. Finley for performing the melt viscosity experiments, and G. S. Schumann for performing the VPO experiment. A special thanks is extended to Dr. K. M. O'Connor for assistance in determining the densities.

References and Notes

(1) Andruzzi, F.; Barone, C.; Lupinacci, D.; Magagnini, P. L. *Makromol. Chem., Rapid Commun.* **1984**, *5*, 603.
(2) Takayanagi, M.; Katayose, T. *J. Appl. Polym. Sci.* **1984**, *29*, 141.
(3) Espenscheid, B.; Schulz, R. C. *Makromol. Chem., Rapid Commun.* **1983**, *4*, 633.
(4) Bannister, D. J.; Doyle, M.; Macfarlane, D. R. *J. Polym. Sci., Polym. Lett. Ed.* **1985**, *23*, 465.
(5) Segre, A. L.; Andruzzi, F.; Barone, C.; Paci, M.; Magagnini, P. L. *J. Polym. Sci., Polym. Phys. Ed.* **1985**, *23*, 2611.
(6) Hackbarth, H.; Ritter, H. *Makromol. Chem., Rapid Commun.* **1986**, *7*, 33.
(7) Rim, P. B. *J. Macromol. Sci., Phys.* **1984**, *B23*, 549.
(8) Rim, P. B.; O'Connor, K. M. *J. Polym. Sci., Polym. Lett. Ed.* **1986**, *24*, 95.
(9) Rim, P. B.; O'Connor, K. M. *J. Appl. Polym. Sci.* **1986**, *32*, 4679.
(10) Rim, P. B. *Polym. Commun.* **1986**, *27*, 199.
(11) Yilgör, I.; McGrath, J. E. *Polym. Bull. (Berlin)* **1984**, *12*, 491.
(12) Yilgör, I.; McGrath, J. E. *Polym. Bull. (Berlin)* **1984**, *12*, 499.
(13) Collins, E. A.; Bares, J.; Billmeyer, F. W., Jr. *Experiments in Polymer Science*; Wiley-Interscience: New York, 1973; Chapter 7.
(14) Newman, S.; Krigbaum, W. R.; Laugier, C.; Flory, P. J. *J. Polym. Sci.* **1954**, *14*, 451.
(15) Spurlin, H. M.; Martin, A. F.; Tennent, H. G. *J. Polym. Sci.* **1946**, *1*, 63.
(16) Ferry, J. D. *Viscoelastic Properties of Polymers*, 3rd ed.; Wiley: New York, 1980; Chapter 12.
(17) Beuche, F. *Physical Properties of Polymers*; Interscience: New York, 1962; Chapter 3.
(18) Dannhauser, W.; Child, W. C., Jr.; Ferry, J. D. *J. Colloid Sci.* **1958**, *13*, 103.
(19) Wunderlich, B. *Macromolecular Physics*; Academic: New York, 1980; Vol. 3, Chapter 10.
(20) Broadhurst, M. G. *J. Res. Natl. Bur. Stand., Sect. A* **1962**, *66A*, 241.
(21) Hsieh, H. W. S.; Post, B.; Morawetz, H. *J. Polym. Sci., Polym. Phys. Ed.* **1976**, *14*, 1241.
(22) Jordan, E. F., Jr.; Feldeisen, D. W.; Wrigley, A. N. *J. Polym. Sci., Polym. Chem. Ed.* **1971**, *9*, 1835.
(23) Hoffman, J. D.; Weeks, J. L. *J. Res. Natl. Bur. Stand., Sect. A* **1962**, *66A*, 13.
(24) Wunderlich, B.; Czornyj, G. *Macromolecules* **1977**, *10*, 906.
(25) Flory, P. J.; Vrij, A. *J. Am. Chem. Soc.* **1963**, *85*, 3548.
(26) Cantor, R. S.; Dill, K. A. *Macromolecules* **1985**, *18*, 1875.
(27) Watanabe, J.; Ono, H.; Uematsu, I.; Abe, A. *Macromolecules* **1985**, *18*, 2141.